Point Sample Rendering

An article by

J.P. Grossman/ W. Dally

presented by

Alexandre Desboeufs

Contents

1. Introduction

In Point Sample Rendering, objects are modeled as a dense set of surface point samples. These samples are obtained from orthographic views and are stored with colour, depth and normal information, enabling Z-buffer composition, Phong shading, and other effects such as shadows. Motivated by image based rendering, point sample rendering is similar in that it also takes as input existing views of an object and then uses these to synthesize novel views. It is different in that (1) the point samples contain more geometric information than image pixels, and (2) these samples are *view independent* - that is, the colour of a sample does not depend on the direction

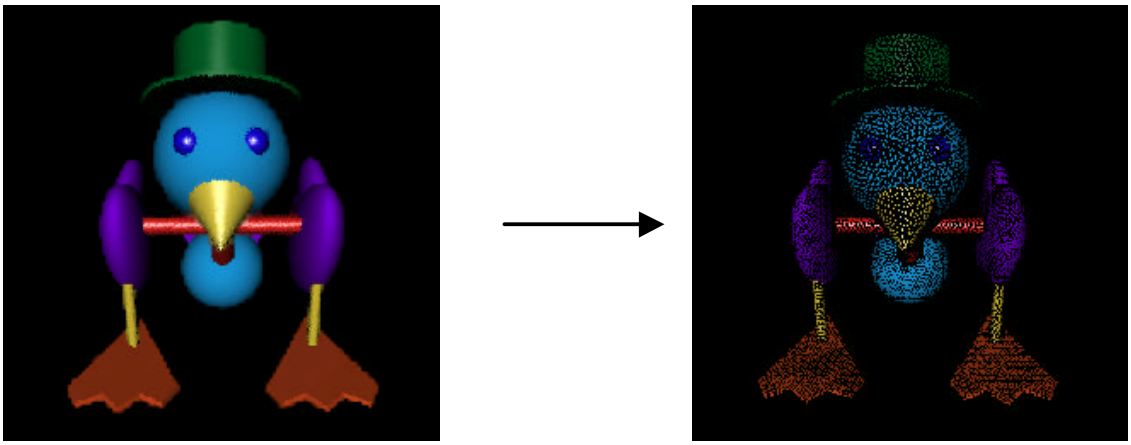

object **point sample representation**

Figure 2.1: Point sample representation of an object.

from which it was obtained.

The use of points as a rendering primitive is appealing due to the speed and simplicity of such an approach. Points can be rendered extremely quickly; there is no need for polygon clipping, scan conversion, texture mapping or bump mapping. Like image based rendering, point sample rendering makes use of today's large memories to represent complex objects in a manner that avoids the large render-time computational costs of polygons. Unlike image based representations, which are view dependent and will therefore sample the same surface element multiple times, point sample representations contain very little redundancy, allowing memory to be used efficiently.

2. Object Sampling

2.1 Mesh of Points

One approach to the problem of surface reconstruction is to treat the point samples as vertices of a triangular mesh which can be scan-converted. We have rejected this approach for a number of reasons. First and foremost, it is slow, requiring a large number of operations per point sample. Second, it is difficult to correctly generate the mesh without some a priori knowledge of the object's surface topology; there is no exact way to determine which points should be connected to form triangles and which points lie on different surfaces and should remain unconnected. Invariably one must rely on some heuristic which compares depths and normals of adjacent points. Third, it is extremely difficult to ascertain whether or not the entire surface of the object is covered by the union of all triangles from all views, especially if we are retaining only a subset of the point samples from each view. Fourth, when a concave surface is sampled by multiple views, the triangles formed by points in one view can obscure point samples from other views (figure 2.2a). This degrades the quality of rendered images by causing pixels to be filled using the less accurate colour obtained from triangle interpolation rather than the more accurate point sample which lies behind the triangle. Fifth, noticeable artifacts result when we attempt to combine triangles from multiple views in a single image. Far from merging seamlessly to form a single continuous surface, triangles from different views appear incoherent, as shown in figure 2.2b.

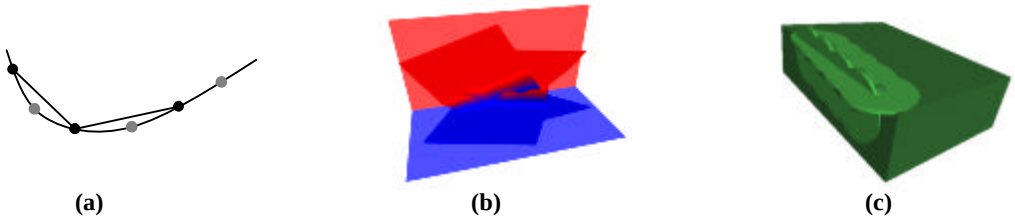

Figure 2.2

Another approach is the use of 'splatting', whereby a single point is mapped to multiple pixels on the screen, and the colour of a pixel is the weighted average of the colours of the contributing points. However, this is again slow, requiring a large number of operations per point. Furthermore, choosing the size and shape of the splat to ensure that there are no tears in any surface is an extremely difficult problem. One interesting idea is to use point sample normals to draw small oriented circles or quadrilaterals, but this results in 'overshoot' near corners as shown in figure 2.2c.

2.2 Adequate Sampling

In order to maximize speed, our solution essentially ignores the problem altogether at render. To see how this can be achieved without introducing holes into the image, we start with the simplifying assumptions that the object will be viewed orthographically, and that the target resolution and magnification at which it will be viewed are known in advance. We can then, in principle, choose a set of surface point samples which are dense enough so that when the object is viewed there will be no holes, independent of the viewing angle. We say that an object or surface is **adequately sampled** (at the given resolution and magnification) if this condition is met.

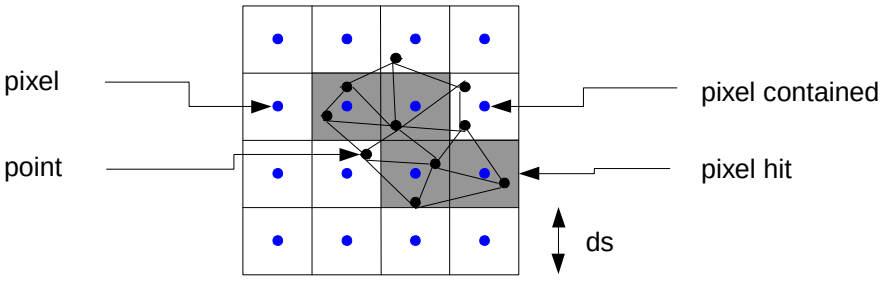

Figure 2.3

We begin by establishing a geometric condition which guarantees that a set of point samples forms an adequate sampling of a surface. Suppose we overlay a finite triangular mesh on top of a regular array of square pixels. We say that a pixel is **contained** in the triangular mesh if its center lies within one of the triangles (figure 2.3). As before, we say that a pixel is **hit** by a mesh point if the mesh point lies inside the pixel.

Theorem If the side length of each triangle in the mesh is less than the pixel side length, then every pixel which is contained in the mesh is hit by some point in the mesh.

Corollary Suppose a surface is sampled at points which form a continuous triangular mesh on the surface. If the side length of every triangle in the mesh is less than the side length of a pixel at the target resolution (assuming unit magnification), then the surface is adequately sampled.

In particular, it suggests that to minimize the number of samples, the distance between adjacent samples on the surface of the object should be as large as possible but less than *ds*, the pixel side length at the target resolution (again assuming unit magnification). In order to obtain such a uniform sampling, we sample orthographic views of the object on an equilateral triangle lattice. Now it is possible for the distance between adjacent samples on the object to be arbitrarily large on surfaces which are nearly parallel to the viewing direction (figure 2.4a). However, suppose we restrict our attention to a surface (or partial surface) S whose normal differs by no more than θ from the projection direction at any point, where θ is a 'tolerance angle'. If we sample the orthographic view on an equilateral triangle lattice with side length $ds \cdot \cos\theta$, we

obtain a continuous triangular mesh of samples on S in which each side length is at most ($ds \cdot \cos\theta$) / $\cos\theta$ = ds (figure 2.4b). Hence, S is adequately sampled.

Rather than sampling the orthographic projections on a square lattice at the target resolution, we sample on a denser equilateral triangle lattice. The density of the lattice is determined by the tolerance angle; if the tolerance angle is θ then the spacing between samples is $ds \cdot \cos\theta$ (where ds is the pixel side length), which gives us $2/\sqrt{3}\cos^2 q$ samples per pixel. We typically use θ = 25° which translates to 1.4 samples per pixel.

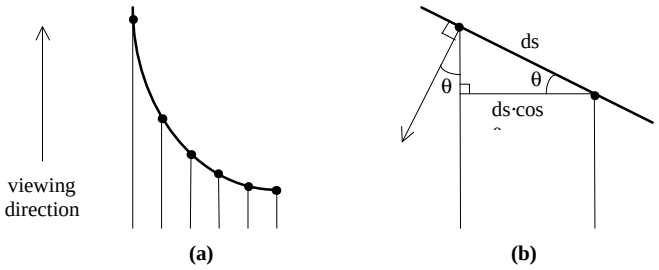

Figure 2.4

2.3 Memory Structure

Each point sample contains a depth, an object space surface normal, diffuse colour, specular colour and shininess. Table 2.5 gives the amount of storage associated with each of these; an entire point will fit into three 32 bit words. Surface normals are quantized to one of 32768 unit vectors (figure 2.6). These vectors are generated using the same procedure described previously to generate projection directions, except that there are 6 levels of subdivision rather than 1, producing 32768 spherical triangles. The vectors are stored in a large lookup table which is accessed when the points are shaded at render time.

Field	**# bits**	**Description**
Depth	32	Single precision floating point
Object space normal	15	quantized to one of 32768 vectors
Diffuse colour	24	8 bits of red, green, blue
Specular colour	16	6 bits of green, 5 bits of red, blue
Shininess	8	Exponent for Phong shading
Total	**95**	

Table 2.5: Data associated with each point sample

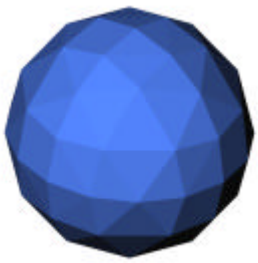

Figure 2.6: The sphere of directions is subdivided into 128 triangles. Each triangle contains a set of directions which is represented by a single bit in the visibility mask.

The samples in a projection are divided into 8x8 blocks. This allows us to compress the database by retaining only those blocks which are needed while maintaining the rendering speed and storage efficiency afforded by a regular lattice (a regular lattice can be rendered quickly by using incremental calculations to transform the points, and it can be stored more compactly than a set of unrelated points as we only need to store one spatial coordinate explicitly). In addition, the use of blocks makes it possible to amortize visibility tests over groups of 64 points.

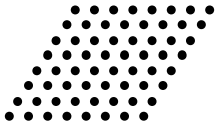

2.4 The Algorithm

The union of point samples from all projections is assumed to form an adequate sampling of the object. The next task in the modeling process is to find a subset S of blocks which is still an adequate sampling but contains as little redundancy as possible. For this we use a greedy algorithm.

We start with no blocks ($S = \phi$). We then step through the list of orthographic projections; from each projection we select blocks to add to S. A block is selected if it corresponds to a part of the object which is not yet adequately sampled by S. Rather than attempt to exactly determine which surfaces are not adequately sampled, which is extremely difficult, we employ the heuristic of both ray tracing the orthographic projection and reconstructing it from S, then comparing the depths of the two images thus obtained (figure 2.7). This tests for undersampled surfaces by searching for pixels which are 'missed' by the reconstruction. If a pixel is missing from a surface then, by definition, that surface is not adequately sampled. However, if no pixels are missing from a surface it does *not* follow that the surface must be adequately sampled, as there may be some other rotated/translated view in which the surface will contain a hole. Thus, to enhance the quality of the test it is repeated several times using various translations and rotations for the view. Typically, we use every combination of four rotations (0°, 22.5°, 45°, 67.5°) and four translations (either no offset or a one half pixel offset in both x and y), a total of sixteen tests.

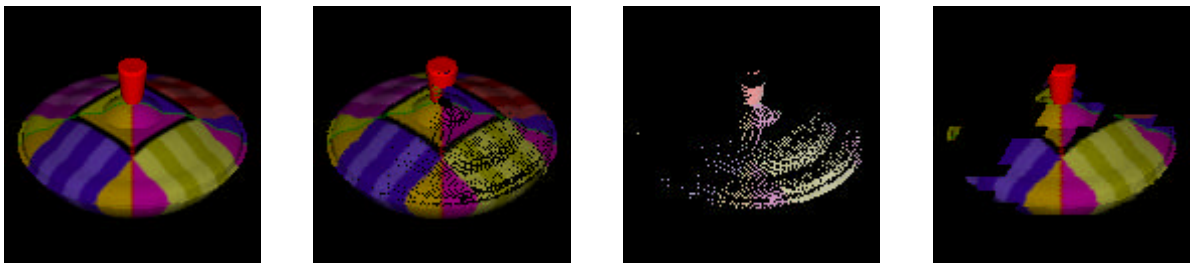

(a) **(b)** **(c)** **(d)**

Figure 2.7: Block Selection. **(a)** Ray traced projection. **(b)** Projection reconstructed from current set of blocks. **(c)** Pixels where (a) and (b) have different depths. **(d)** Blocks added to set.

Since we start with no blocks, there will be a bias towards including blocks from earlier projections. Indeed, for the first two projections, which are taken from opposite directions, all the blocks which contain samples of the object will necessarily be included. To eliminate this bias we make a second pass through the projections in the same order; for each projection we remove from S any of its blocks that are no longer needed. This second pass has been observed to decrease the total number of blocks in the set by an average of 22%.

2.5 Magnification / Perspective

The concept of an 'adequately sampled' surface does not solve the surface reconstruction problem; if we wish to magnify the object we are once again confronted by the original dilemma. However, suppose that the object is adequately sampled at the original resolution/magnification, and suppose we decrease the image resolution by the same amount that the magnification is increased. The object will again be adequately sampled at this new resolution/magnification. Thus, we can render the object at the lower resolution and resample the resulting image to the desired resolution.

This works well for reconstructing orthographic views of the object, but when we try to adapt the solution to perspective views we encounter a problem: because of the perspective transform, different parts of the object will be magnified by different amounts. A straightforward solution would be to choose a single lower resolution taking into account the *worst case* magnification of the object, i.e. the magnification of the

part closest to the viewer. However, this unfairly penalizes those parts of the object which would be adequately sampled at a higher resolution, and it unnecessarily degrades the quality of the final image.

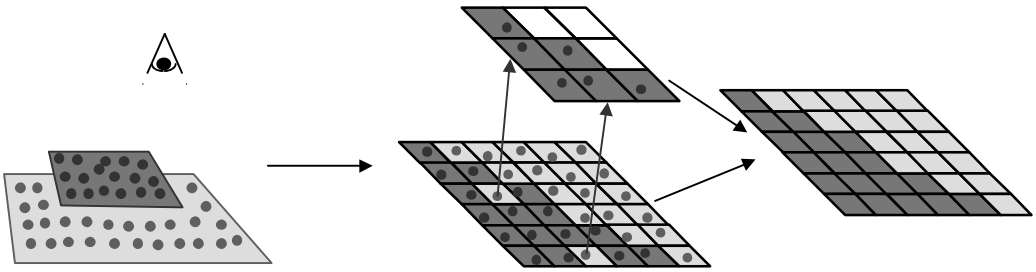

Figure 2.8: The dark surface is rendered using a higher level depth buffer in which there are no gaps. This depth buffer is used to detect and eliminate holes in the image.

To address this problem, we introduce a *hierarchy* of lower resolution depth buffers as in [Green93]. The lowest buffer in the hierarchy has the same resolution as the target image, and each buffer in the hierarchy has one half the resolution of the buffer below. Then, in addition to mapping point samples into the destination image as usual, each part of the object is rendered in a depth buffer at a low enough resolution such that the points cannot spread out and leave holes. When all parts of the object have been rendered, we will have an image which, in general, will contain many gaps. However, it is now possible to detect and eliminate these holes by comparing the depths in the image to those in the hierarchy of depth buffers (figure 2.8). The next two sections provide details of this process.

3. Rendering

3.1 Visibility Testing

The first method which is used to test a block's visibility is to see if it lies within the **view frustum** – the region of space that is in the camera's field of view. As usual, the view frustum is defined by a 'near' plane, a 'far' plane, and the four planes which pass through the camera and the sides of the screen (figure 3.1). We use a block's bounding sphere to determine whether or not the block lies entirely outside one of these planes. If it does, then we don't need to render it.

If a block lies inside the view frustum, then whether or not it is visible depends on whether or not it is obscured by some other part of the object, which in turn depends on the position of the camera. A brute force approach to determining visibility, then, is to subdivide space into a finite number of regions and to associate with each region a list of potentially visible blocks. However, we chose not to implement a visibility test based on spatial subdivision due to the large amount of storage required. Since this is a three dimensional problem, the number of bits of storage which are needed is proportional to the number of blocks times the cube of the resolution of the spatial subdivision.

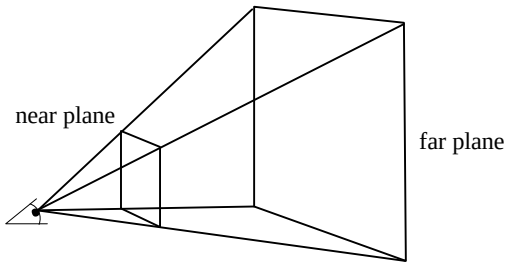

Figure 3.1: View Frustum

One way to lessen the amount of storage required is to reduce the dimensionality of the problem. If we restrict our attention to viewpoints which lie outside the convex hull of the object, then whether or not a block is visible depends only on the *direction* from which it is viewed. Visibility as a function of direction is a two dimensional problem which we tackle using **visibility masks.**

To compute the visibility masks, we render the entire set of blocks orthographically from a number of directions in each triangle (typically ten directions per triangle). Each point is tagged with a pointer to its block; this tag is used to determine the subset of blocks which contribute to the orthographic images. The visibility masks in this subset of blocks are updated by setting the appropriate triangle bit.

The simplest way to make use of these masks at render time is to construct a visibility mask for the screen. In this mask, the k^{th} bit is set if and only if some direction from a screen pixel to the eye lies inside the k^{th} triangle on the triangulated sphere of directions. We then AND this mask with each block's mask; a block is definitely not visible if the result of this test is zero (illustrated in two dimensions in figure 3.2).

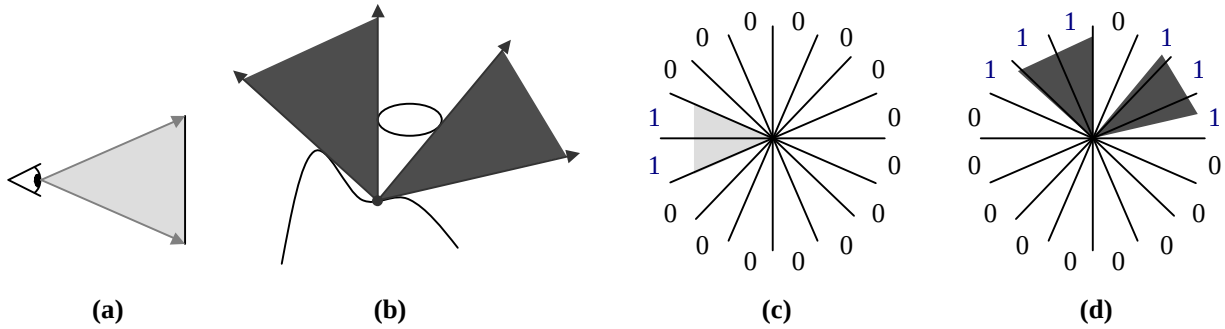

Figure 3.2: Using visibility masks to test visibility. **(a)** Eye-screen directions. **(b)** Set of directions from which a point is visible. **(c)** Screen mask generated from set of screen-eye directions. **(d)** Visibility mask of point. We can deduce that the point is not visible from the fact that the AND of the two masks is zero.

One of the basic visibility tests used in polygon rendering is "backface culling"; there is no need to render polygons whose normals are pointing away from the viewer. We can adapt this test to point sample rendering. We begin with the observation that, similar to polygons, the tangent plane at each point sample defines a half space from which the point is never visible. Taking the intersection of these half spaces over all the points in a block, we obtain a region in space, bounded by up to 64 planes, from which no part of the block is ever visible. It would be quite expensive to attempt to exactly determine whether or not the camera lies inside this region. Instead, we can approximate the region by placing a cone inside it. This **visibility cone** gives us a fast, conservative visibility test; no part of the block is visible from any viewpoint within the cone.

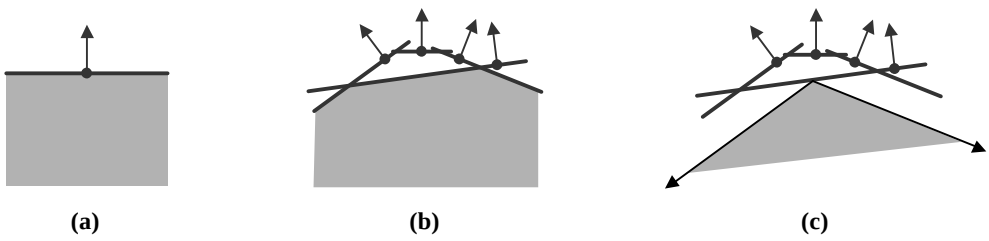

Figure 3.3: Visibility cone in two dimensions. **(a)** Half space from which point is never visible. **(b)** Region from which no part of the block is visible. **(c)** Cone inside region.

3.2 Block Warping

In this section we will describe the basic Point Sample Rendering algorithm which maps each point sample to the nearest pixel in the destination image. We will show how the computations can be optimized using incremental calculations. We ignore for the time being the hierarchical Z-buffer which will be discussed in section chapter 2.5.

Recall that the points in a block are stored in the coordinates of the orthographic projection from which the block was obtained. We begin, then, by computing, for each projection, the transformation from projection space to *camera space.* By camera space we mean the coordinate system in which the camera is at the origin and the screen is a square of side 2 centered and axis-aligned in the plane $z = 1$. We can write this transformation as

$$\begin{bmatrix} x' \\ y' \\ z' \end{bmatrix} = \mathbf{A}\begin{bmatrix} x \\ y \\ z \end{bmatrix} + \mathbf{v} = \begin{bmatrix} A_{xx} & A_{xy} & A_{xz} \\ A_{yx} & A_{yy} & A_{yz} \\ A_{zx} & A_{zy} & A_{zz} \end{bmatrix}\begin{bmatrix} x \\ y \\ z \end{bmatrix} + \begin{bmatrix} v_x \\ v_y \\ v_z \end{bmatrix}$$

where (x, y, z) are the projection space coordinates of a point, (x', y', z') are the camera space coordinates, **A** is an orthogonal matrix giving the rotation and scale components of the transformation, and **v** is a translation vector. We can then compute the integer screen coordinates (u, v) from the camera space coordinates with a perspective divide and a scale/offset which maps [-1, 1] to [0, N] as follows:

$$u = \left\lfloor \frac{N}{2}\left(\frac{x'}{z'}+1\right)\right\rfloor \qquad v = \left\lfloor \frac{N}{2}\left(\frac{y'}{z'}+1\right)\right\rfloor$$

In order to implement the surface reconstruction algorithm presented in chapter 2.5, each block must be warped into the hierarchy of Z-buffers at a low enough resolution such that its points can't spread out and leave holes. If the image resolution is NxN, then the k^{th} depth buffer has resolution $\left\lceil \frac{N}{2^k} \right\rceil \times \left\lceil \frac{N}{2^k} \right\rceil$ where $\lceil \cdot \rceil$ denotes the least integer function. To select an appropriate depth buffer for the block, we start with the assumption that the block is an adequate sampling for orthographic views with unit magnification at MxM pixels. Suppose that the object is being rendered with magnification g and let $d = \min_i z_i'$ where z_i' is the camera space depth of the i^{th} point in the block as before. Then the worst case effective magnification of the block, taking into account the change in resolution, the object magnification, and the perspective projection, is

$$\frac{gN}{Md}$$

To compensate for this, we need to choose the depth buffer such that $\frac{gN}{Md2^k} \le 1$

Thus, we take $k = \max\left(0, \left\lceil \log\left(\frac{gN}{Md}\right)\right\rceil\right)$

It is fairly expensive to compute $d = \min_i z_i'$ exactly. As an approximation, we can instead use the distance d' from the camera to the bounding sphere of the block. This provides a lower bound for d and is much easier to calculate.

If $k = 0$, then the block is being warped into the usual depth buffer. If $k > 0$, then we need to augment the warping procedure as follows:

```
for each point
   compute u, v, z'
   if (z' < depth(0, u, v))
         depth(0, u, v) = z'
         copy point to pixel(u, v)
         u' = u/2^k
         v' = v/2^k
         if (z' + threshold < depth(k, u', v'))
               depth(k, u', v') = z' + threshold
   end if
end for
```

where `depth(k, u, v)` denotes the k^{th} Z-buffer depth at (u, v).

Note that instead of simply testing the point's Z value against the value in the depth buffer, we first add a small threshold. The reason for this is that the depth buffer will be used to filter out points which lie behind the foreground surface; the use of a threshold prevents points which lie *on* the foreground surface from being accidentally discarded. For example, suppose 3 points from a foreground surface and 1 point from a background surface are mapped to four different image pixels contained in a single depth map pixel (shown in one dimension in figure 3.4). Without the threshold, all but the nearest of these points will be discarded (figure 3.4a). The use of a threshold prevents this from happening (figure 3.4b), allowing us to use all or most of the surface points when computing the final image. We found a good choice for the threshold to be

three times the image pixel width; smaller thresholds produce images of lower quality, while larger thresholds begin to have difficulty discriminating between foreground and background surfaces. Figure 3.5 shows the striking difference in image quality which results from the use of a threshold; the left image was rendered using a threshold of three times the image pixel width.

(a) **(b)**

Figure 3.4: Four points are mapped to different image pixels contained in a single depth map pixel. **(a)** No depth threshold - only the nearest point is retained. **(b)** The use of a small threshold prevents points on the same surface as the nearest point from being discarded

Figure 3.5: Depth no threshold (left) vs. Threshold (right).

3.3 Finding Gaps

The easiest way to use the hierarchical depth buffer to detect holes is to treat a pixel in the k^{th} depth buffer as an opaque square which covers exactly 4^k image pixels. We can then make a binary decision for each pixel by determining whether or not it lies behind some depth buffer pixel. If a pixel is covered by a depth buffer pixel, then we assume that it does not lie on the foreground surface, i.e. it is a hole. In the final image this pixel must be recoloured by interpolating its surroundings. If a pixel is *not* covered by any depth buffer pixels, then we assume that it *does* lie on the foreground surface, and its colour is unchanged in the final image. This method is fast and easy to implement. However, it produces pronounced blocky artifacts, particularly at edges, as can be seen in figure 3.6-up.

Our strategy for dealing with this problem is to replace the binary decision with a continuous one. Each pixel will be assigned a weight in [0, 1] indicating a 'confidence' in the pixel, where a 1 indicates that the pixel is definitely in the foreground and a 0 indicates that the pixel definitely represents a hole and its colour should be ignored. The weights will then be used to blend between a pixel's original and interpolated colours. To see how these weights can be obtained, we observe that: (i) if a pixel is surrounded by depth buffer pixels which are closer to the viewer, then it is certainly a hole and should have weight 0; (ii) if a pixel is surrounded by depth buffer pixels which are further away from the viewer, then it is certainly in the foreground and should have weight 1; (iii) if a pixel is surrounded by depth buffer pixels both closer to and further away from the viewer, then it lies near the edge of the surface and should have a weight between 0 and 1. It therefore makes sense to consider *multiple* depth buffer pixels when assigning a weight to a single image pixel.

In figure 3.6-down shows the weights that are assigned to image pixels using bilinear interpolation. These weights are used to blend between each pixel's original and interpolated colours; in the final image the artifacts are much less prominent (3.6-up).

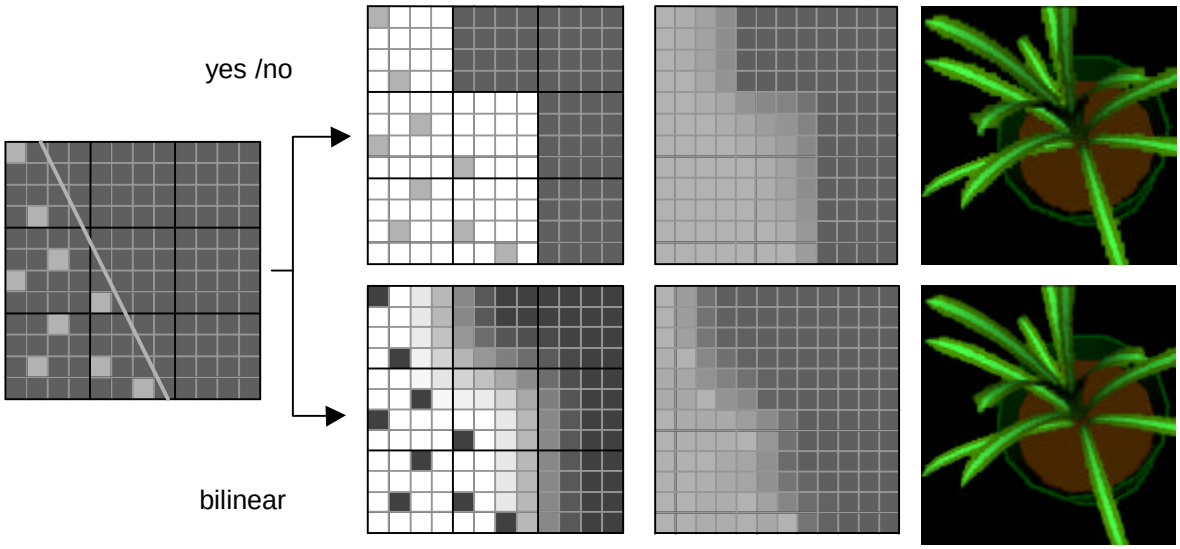

Figure 3.6: (up) the simple method, (down) the bilinear method

3.4 Shadows

Shadows are computed using shadow maps. For each light, we render the object from the light's viewpoint and use a hierarchical depth map to store Z values. Since we are *only* interested in creating a depth map, we don't have to worry about copying points' reflectance information into a destination image. The warping procedure is thus greatly simplified. For each block we again choose an appropriate level *k* in the depth buffer hierarchy and then warp the points as follows:

```
for each point
  compute u', v', z'
  if (z' < depth(k, u', v'))
        depth(k, u', v') = z'
  end if
end for
```

To calculate how much of a given point is in shadow, we first transform the point to *light space*, the coordinate system of the light's hierarchical depth map. We then compute a coverage for the point using almost exactly the same procedure as that used in section 3.3 for detecting gaps. The only difference is that we subtract a small bias from the point's depth before comparing it to the depths in the shadow map, to prevent surfaces from casting shadows on themselves due to small inaccuracies in the computation of the points' light space coordinates. In our case, these inaccuracies arise primarily from the fact that the points' *x'* and *y'* camera space coordinates are rounded to pixel centers.

Since the warping procedure used to create shadow maps is so simple, it is extremely fast. As a result, shadows can be computed with much less overhead than would normally be expected from an algorithm which re-renders the object for each light source. For example, figure 3.7 was rendered at 256x256 pixels with three light sources - two directional lights and a spotlight. It took 204ms to render without shadows and 356ms with shadows - an overhead of less than 25% per light source.

Figure 3.7: Fast shadows.

3.5 Filing Gaps / Shading

To fill the gaps in the final image we must compute a colour for pixels with weight less than 1. This problem is not specific to point sample rendering; it is the general problem of image reconstruction given incomplete information. In the 'pull' phase we compute a succession of lower resolution approximations of the image, each one having half the resolution of the previous one. In the 'push' phase, we use these lower resolution images to fill gaps in the higher resolution images. This is illustrated in figure 3.8 with a picture of a mandrill.

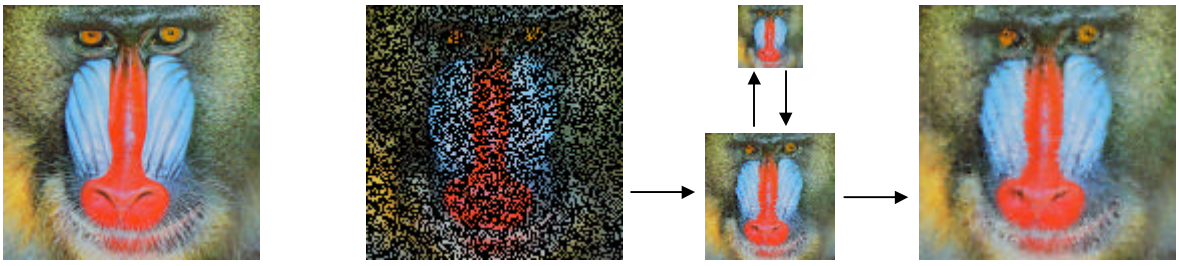

(a) **(b)** **(c)** (d)

Figure 3.8: The pull-push algorithm. **(a)** Original image. **(b)** Incomplete image; 50% of the pixels have been discarded. **(c)** Lower resolution approximations. **(d)** Reconstruction.

The lower resolution approximations of the image are computed by repeatedly averaging 2x2 blocks of pixels, taking the weight of the new pixel to be the sum of the weights of the four pixels, capped at 1. Specifically, if $c^k_{x,y}$ and $w^k_{x,y}$ are the colour and weight of the (x, y) pixel in the k^{th} low resolution approximation, then:

$$c^{k+1}_{x,y} = \frac{w^k_{2x,2y}c^k_{2x,2y} + w^k_{2x+1,2y}c^k_{2x+1,2y} + w^k_{2x,2y+1}c^k_{2x,2y+1} + w^k_{2x+1,2y+1}c^k_{2x+1,2y+1}}{w^k_{2x,2y} + w^k_{2x+1,2y} + w^k_{2x,2y+1} + w^k_{2x+1,2y+1}}$$

$$w^{k+1}_{x,y} = MIN(1,\quad w^k_{2x,2y} + w^k_{2x+1,2y} + w^k_{2x,2y+1} + w^k_{2x+1,2y+1})$$

In the 'push' phase, to compute the final colour $c'^k_{x,y}$ of the (x, y) pixel in the k^{th} low resolution image, we inspect its weight $w^k_{x,y}$. If $w^k_{x,y} = 1$ then we simply set $c'^k_{x,y} = c^k_{x,y}$. Otherwise, we compute an interpolated colour $\tilde{c}^k_{x,y}$ using as interpolants the pixels in the $(k+1)^{\text{st}}$ image. We then set

$$c'^k_{x,y} = w^k_{x,y}c^k_{x,y} + (1 - w^k_{x,y})\tilde{c}^k_{x,y}$$

If we were to use bilinear interpolation to compute $\tilde{c}^k_{x,y}$, then we would interpolate the four closest pixels in the $(k+1)^{\text{st}}$ image with weights 9/16, 3/16, 3/16 and 1/16 (since the interpolation is always from one level up in the hierarchy, the weights never change). However, if we approximate these weights as ½, ¼, ¼ and 0, then the algorithm runs significantly faster (over 6 times faster using packed RGB arithmetic; see Appendix) without any noticeable degradation in image quality. Hence, we interpolate the three closest pixels in the $(k+1)^{\text{st}}$ image with weights ½, ¼ and ¼. For example,

$$\tilde{c}^k_{2x+1,2y+1} = \frac{1}{2}c'^{k+1}_{x,y} + \frac{1}{4}c'^{k+1}_{x+1,y} + \frac{1}{4}c'^{k+1}_{x,y+1}$$

with similar expressions for $\tilde{c}^k_{2x,2y}$, $\tilde{c}^k_{2x+1,2y}$, and $\tilde{c}^k_{2x,2y+1}$.

3.6 Filing Gaps

After all the blocks have been warped and weights have been assigned to image pixels as described in section 3.3, the non-background pixels with positive weight must be shaded according to the current lighting model. Performing shading in screen space after pixels have been weighted saves time by shading only those points which contribute to the final image. For our purposes the lighting model is Phong shading with shadows, but one could certainly implement a model which is more or less sophisticated as needed.

Since point sample normals are stored in object space, we perform shading calculations in object space to avoid transforming the normals to another coordinate system. We therefore need to recover object space coordinates for the points contained in the image pixels. Since we do not store the exact camera space *x'* and *y'* coordinates for points when they are copied to pixels in the image buffer, we assume that they are located at the pixel centers. Using the *z'* coordinates which are stored in the image Z-buffer, we can then transform the points from camera space to object space. The pixel centers form a regular square lattice, so this transformation can be done quickly using incremental calculations.

It is worth noting that because of the dense reflectance information contained in point sample models, the resulting specular highlights are of ray-trace quality, as can be seen in figure 3.9.

Figure 3.9: High quality specular highlights.

4. Conclusion

Point Sample Rendering is an algorithm which features the speed of image based graphics with quality, flexibility and memory requirements approaching those of traditional polygon graphics. Objects are represented as a dense set of point samples which can be rendered extremely quickly. These point samples contain precise depth and reflectance information, allowing objects to be rendered in dynamically lit environments with no geometric artifacts. Because the point samples are view-independent, point sample representations contain very little redundancy, allowing memory to be used efficiently.

A novel solution to the problem of surface reconstruction has been introduced, using a combination of adequate sampling and hierarchical Z-buffers to detect and repair surface tears. This approach does not sacrifice the speed of the basic rendering algorithm, and in certain cases it guarantees that images will not contain holes. It also been shown how a variant of percentage closer filtering can be used to eliminate artifacts which result from a straightforward utilization of the hierarchical Z-buffer.

Because of its flexibility, Point Sample Rendering is suitable for modeling and rendering complex objects in virtual environments with dynamic lighting such as flight simulators, virtual museums and video games. It is also appropriate for modeling real objects when dense reflectance information is available. Since Point Sample Rendering has low memory requirements, it can be implemented on inexpensive personal computers.

The authors have shown that it is possible to render directly from point samples. The software system, implemented on a 333MHz Pentium II, has demonstrated the ability of Point Sample Rendering to render complex objects in real time. It has also shown that the resulting images are of high quality, with good shadows and ray-trace quality specular highlights.

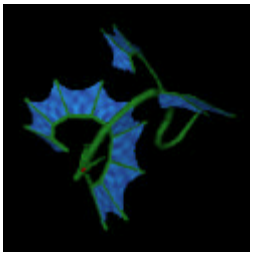

Dragon

Kittyhawk

Toybird

Pine Tree

	Dragon	Kittyhawk	Toybird	Pine Tree
File Size (in mega byte))	0.96	1.73	1.46	7:12
Number of blocks	2100	3390	2411	11051
Construction time (h : m)	00:18	01:02	00:11	01:35
Rendering time (in ms on a 333 Mhz Pentium II)				
Init	10	10	9	10
Visibility	3	5	9	4
Warp	36	62	226	50
Find gaps	7	8	4	8
Shade	18	23	25	23
Pull	7	7	7	7
Push	3	3	2	3
Total	84	118	282	105